

INJECTION SYSTEM FOR KHARKOV X-RAY SOURCE NESTOR

P. Gladkikh, I. Karnaukhov[#], A. Mytsykov, A. Zelinsky, National Science Center “Kharkov Institute of Physics and Technology”, Kharkov, Ukraine

Abstract

During the last three years a Kharkov X-ray generator NESTOR is under design and construction in NSC KIPT. According to the design report, electrons are injected in the storage ring at 100 MeV and ramped up to final energy 225 MeV. Due to compact design of the ring the injection trajectory of the beam will pass through fringe field of a NESTOR bending magnet. It brings additional difficulties on design of an injection channel.

In the paper the layout, results of design and calculations of NESTOR injector channel are presented. The channel consists of two bending magnets, five-lens, asymmetrical, objective and two-lens matching cell to compensate dispersion and focusing effects of a dipole magnet fringe field and injection system elements (inflexor). Presented results shows that designed lattice provides matching of injected beam parameters with the storage ring acceptance, is stable to element alignment errors and is easy controlled. The final values of the channel lens gradients can be defined only after measurements of inflector field profile.

REFERENCE ORBIT DISTORTIONS

A storage ring NESTOR has racetrack like lattice [1]. The lattice consists of 4 bending magnets, 20 quadrupole magnets 18 sextupole magnets partly with octupole field component. A large number of focusing electromagnetic elements and presence of low- β sections demand very strict requirements to the accuracy of lattice element alignment. Reference orbit (RO) distortions have to allow electron beam injection in the storage ring and further RO corrections.

Results of RO numerical simulations at Gaussian distribution of alignment errors of quadrupole lenses with RMS value of alignment errors equal to $\Delta x = \Delta z = 100 \mu\text{m}$ are shown in Fig. 1,2. Fig. 1 shows distribution of maximal RO distortions depends on RMS value of alignment tolerance. Fig. 2 presents dependence of maximum value of RMS RO distortions on RMS value of alignment tolerance.

As calculations showed, the strong lenses of final triplets make the main contribution in RO distortions due to quadrupole lenses misalignments. Because of this the final triplet will be installed in the following way. Firstly lens will be assembled on a solid platform with linear accuracy $\Delta x = \Delta z = 50 \mu\text{m}$ and angle accuracy $\Delta\varphi = 3 \times 10^{-4}$ on all planes. Such preliminary positioning will be made at a magnetic measurement bench. Then the platform with the triplet will be aligned at the ring with linear accuracy $\Delta x = \Delta z = 100 \mu\text{m}$ and angle accuracy $\Delta\varphi = 3 \times 10^{-4}$.

In a similar manner the calculations of RO distortions due to bending magnets misalignments on all planes were carried out (Fig 3). As it is clear from the Fig.1, 2 the contribution of quadrupole lenses in total RO distortion is

much bigger compare to bending magnets misalignment effect.

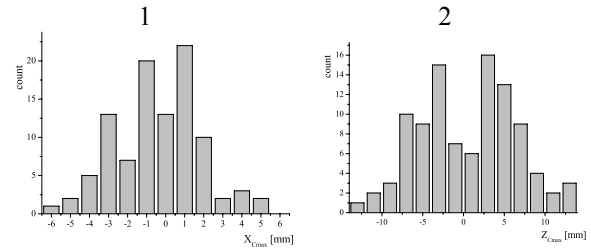


Figure 1: Distribution of maximal value of RO distortions at RMS quadrupole misalignments $\Delta x = 100 \mu\text{m}$: 1 – horizontal plane, 2 – vertical plane.

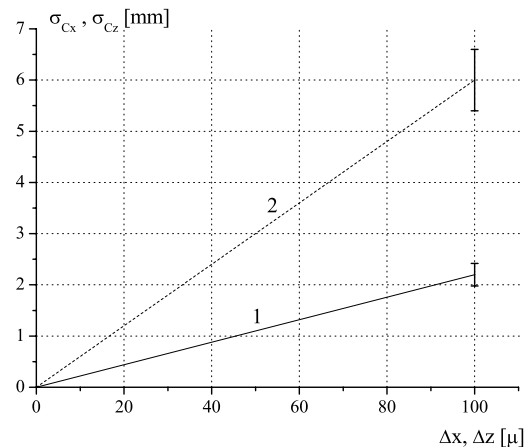


Figure 2: RMS value of maximal RO distortions vs RMS value of quadrupole misalignments in horizontal (1) and vertical (2) planes.

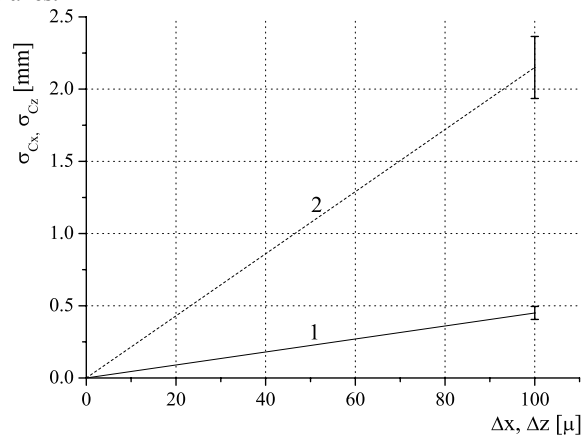


Figure 3. RMS value of maximal RO distortions vs RMS value of bending magnet misalignments in horizontal (1) and vertical (2) planes.

The accuracy of quadrupoles positioning on angle coordinates in planes zx and zs is 0.3 mrad as well angle for bending magnets in the same planes. The accuracy of equipment alignment relative to vertical axis is determined by accuracy of plane measurements and

length of elements. For bending magnets it is $\alpha_{sx} \sim 2.5 \times 10^{-4}$, and for quadrupoles $\alpha_{sx} \sim 1.5 \times 10^{-3}$.

Dependences of RO distortions presented above determined the following tolerances of magnetic element alignments (RMS):

- Accuracy of plane and angular alignment of bending magnet and quadrupoles of regular part of the storage ring $\Delta x = \Delta z = 100 \mu\text{m}$, $\Delta\varphi = 3 \times 10^{-4}$;
- Accuracy of plane alignment of final triplet on the separate solid platform $\Delta x = \Delta z = 50 \mu\text{m}$ and angle accuracy $\Delta\varphi = 3 \times 10^{-4}$ on all planes;
- Accuracy of angular alignments of bending magnets relatively axes $\alpha_{xz} = \alpha_{sx} = \alpha_{zs} \sim 3 \cdot 10^{-4}$;
- Accuracy of angular alignments of quadrupoles of regular part of the ring $\alpha_{xz} = 5 \times 10^{-4}$, $\alpha_{sx} = 1.5 \times 10^{-3}$, $\alpha_{zs} = 5 \times 10^{-4}$;
- Accuracy of plane and angular alignments of solid platforms with the final triplets is $\Delta x = \Delta z = 100 \mu\text{m}$, $\Delta\varphi = 3 \times 10^{-4}$ on all planes.

In Fig. 4 the RMS distortions of RO at accepted tolerances of magnetic elements alignments are presented. As it is clear from the picture the maximal RO distortions are $\sigma_{Cx} \ll X_{ap}$, $3 \sigma_{Cx} \approx Z_{ap}$. (Vacuum chamber aperture can be described as ellipse with semi axes $X_{ap} = 35 \text{ mm}$, $Z_{ap} = 14 \text{ mm}$)

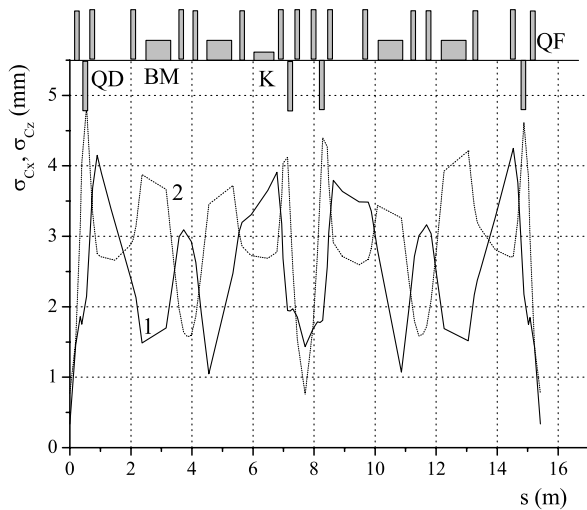


Figure 4: Total RMS distortions in horizontal (1) and vertical (2) planes.

LOCAL CORRECTIONS

It is supposed that ferrite inflector will be used as injection kicker in the NESTOR injection system. Actually this device is pulse septum-magnet with a slit in a septum knife for injected beam extraction. The height of the slip is equal to $\pm 4 \text{ mm}$ and it determines the maximal acceptable value of RO distortions in vertical plane at the injection azimuth. As it can be seen from Fig. 4 the values of RMS RO distortions is approximately equal to 4 mm. It makes injection difficult for realization. For successful injection in the storage ring local correction of RO is needed. The value of orbit bump will

be chosen at the facility tuning and its parameters have to satisfy the following conditions:

- Provide necessary orbit displacements on coordinate Y_i and angle Y'_i at injection azimuth;
- Do not perturb RO out of the pump.

To satisfy these conditions it is necessary to use 4 correctors with fields which values are determined from equations [3].

Local correction of RO at injection azimuth will be carried out with correction coils are placed on sextupoles next to the both side of the inflector. The same correctors will be used for global corrections of RO over the storage ring circumference. Simulations of the RO corrections show that maximal value of corrector strength is $\sim 10 \text{ mrad}$, which needs correcting field $B_j < 200 \text{ Gs}$ at corrector length equal to $L_j = 0.1 \text{ m}$ for maximal orbit distortions equal to $\Delta Z_C = 8 \text{ mm}$.

BEAM TRANSPORTATION TROUGH BENDING MAGNET FRINGING FIELD

At electron beam transportation from a linear accelerator exit to the storage ring the beam will pass through fringing field of the first bending magnet inside the special screen channel [4]. Minimal distance from RO we can place screen made of magnetic material is determined by acceptable value of magnetic field perturbations. Calculations show that this distance can not be less than 0.14 m, here magnetic field change at RO is not more than 5 Gs.

Injection will be carried out at the flat part of inflector field distribution with value of betatron oscillation amplitude in the horizontal plane equal to $X_i = 16 \text{ mm}$, here the optimal injection angle is $\sim 3.6 \text{ mrad}$. Here for calculations electron beam size at injection azimuth were taken equal to the beam size at the linear accelerator exit, i.e. $\sim 1 \text{ mm}$ and $\sim 1 \text{ mrad}$ (beam emittance is 10^{-6}). Effective length of one inflector block is 18 cm, as it follows from field calculations. Inflector will be made of 3 blocks 2 of which will generate field $B_f = 0.035 \text{ T}$ with 5 ns back front. The third block (entrance block for the electron beam) will generate field $B_i = 0.04 \text{ T}$. There are no restrictions for its front duration because particle pass through its field only once.

INJECTION CHANNEL

To provide parallelism of injection section of the ring with the linear accelerator axis the injection channel has to be almost parallel transition lattice with bending angles φ_{B1} and $\varphi_{B2} = -\varphi_{B1} + \varphi_{inj}$. We choose bending angle in the first magnet of the channel $\varphi_{B1} = 60^\circ$. As base lattice for the transportation channel we used classical 5 lenses variant of the lattice [3], which has flexible focusing properties.

The final part of the injection channel i.e. inflector, quadrupole of the storage ring and fringing field of the bending magnet is non dispersion free system. So, transportation channel has to compensate this dispersion.

One can determine this dispersion by transportation of a particle with energy deviation in opposite direction from injection azimuth to the end of the magnetic screen. Calculations show that the parallel transition has to provide the dispersion equal to $D = 0.176 M$ and its derivation $D' = -0.754$ at the magnetic screen exit. In Fig. 5 the results of the injection channel calculations for angles $\varphi_{B1} = 60^\circ$, $\varphi_{B2} = -60^\circ$ with focusing properties providing beam sizes matching are shown. In Fig. 6 phase ellipses of injected beam in the both planes at the exit of magnetic screen are shown. As it can be concluded from the picture comparison, injection channel provides electron beam transition with required beam parameters from the exit of the linear accelerator to the injection azimuth in the storage ring.

Calculations of the channel lattice responsivity for power supply instability and electromagnetic elements misalignments has been carried out. Calculations showed that at power supply instability value equal to $\sim 10^{-3}$ and alignment errors $\sim 200 \mu\text{m}$ and 200 mrad in the both planes the maximal deviation of the beam centroid is of about $\sim 2.5 \text{ mm}$. This deviation can be corrected with 4 pairs of correctors which will be placed as it is shown in Fig. 7.

CONCLUSION

In the paper the results of calculations of the injection system for Kharkov X-ray source on the base of Compton scattering NESTOR are presented. Designed scheme provides transportation of the electron beam with required parameters from the linear accelerator to the entrance in the first bending magnet of the ring and provides effective beam injection to the ring.

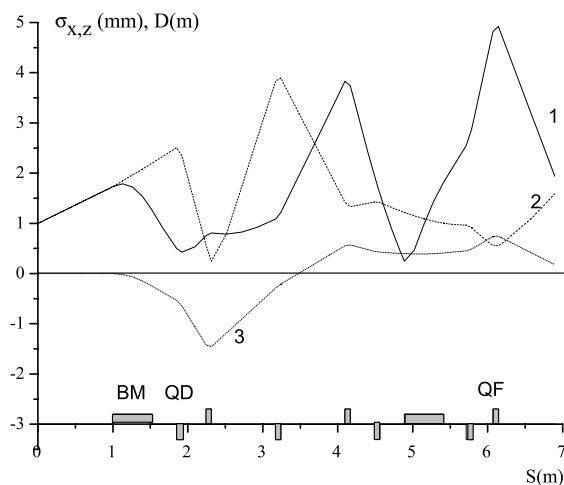


Figure 5: Horizontal (1) and vertical (2) beam envelopes and dispersion function (3) in the injection channel.

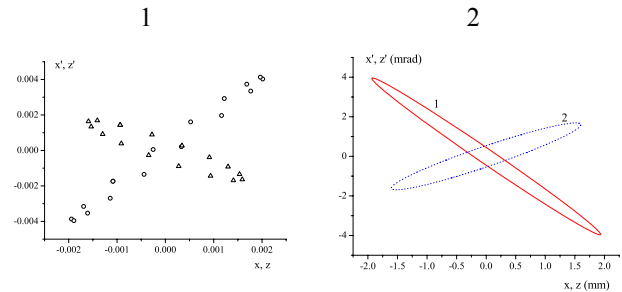


Figure 6. Phase ellipse of the beam produced with beam transportation trough fringing field of the bending magnet (1) and trough transportation channel (2).

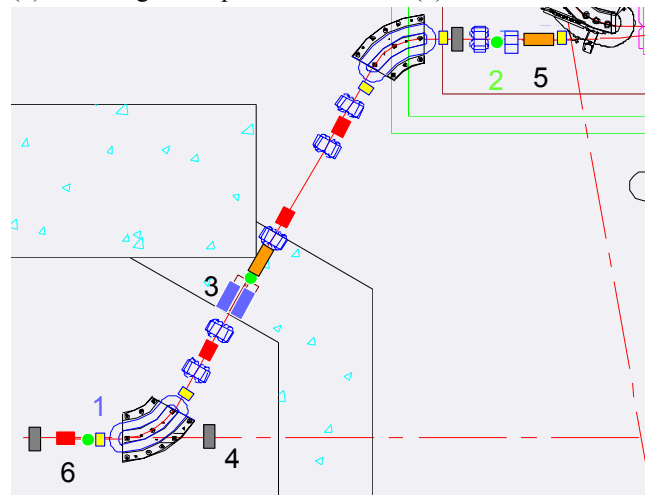


Figure 7. NESTOR injection channel layout: 1 – bellows joint, 2 – pumping points, 3 – collimator, 4 – vacuum valve, 5 – beam position monitor, 6 – beam correctors.

REFERENCES

- [1] V. Androsov et al. "Progress in Development of Kharkov X-Ray Generator NESTOR," Proc. Of FEL'05, 21-26 August, 2005, Stanford USA, pp. 476-479.
- [2] V. Ivashchenko et al. "NESTOR reference orbit correction" Proc. Of EPAC'04, 5-9 July, 2004, Lucerne Switzerland, pp. 1431-1433.
- [3] H. Wiedemann, Particle Accelerator Physics I, Springer, Second Edition.
- [4] A. Zelinsky and A. Mytsykov, "3D Magnetic Field Effects in an NSC KIPT Compact Intense X-ray Generator," Proc. Of SRI 8th conference, 23-29 August, 2003, San Francisco, USA, 2003, p. 129-132.